Biophysical Chemistry 26 (1987) 225–233
Elsevier

BPC 01141

Influence of solvent, anion and presence of nitrogen in the ring structure on the mechanism of complexation of alkali metal cations with crown ethers

George W. Gokel [a], Luis Echegoyen [a], Min Sook Kim [a], Edward M. Eyring [b] and Sergio Petrucci [c]

[a] *Department of Chemistry, University of Miami, Coral Gables, FL 33124,* [b] *Department of Chemistry, University of Utah, Salt Lake City, UT 84112 and* [c] *Department of Chemistry, Polytechnic University, Long Island Center, Farmingdale, NY 11735, U.S.A.*

Accepted 27 February 1987

Complexation kinetics; Lariat crown ether; Solvent effect; Anion effect; Ultrasonic absorption

The mechanism of complexation of alkali metal cations with macrocyclic ligands such as the simple crown ethers and the role of desolvation vs. ligand rearrangement are discussed. The unique role of water solvent in the rate-determining step of complexations in aqueous solutions is brought into focus. The competitive role of the anion, which becomes of paramount importance in solvents of low permittivity, is reiterated. Monoazo crown ethers are shown to possess isomeric equilibria in methanol solvent. The rate-determining process for the first step of complexation of these macrocycles with Na^+ in methanol appears to be the rearrangement of the ligand through inversion to an exo position of the nitrogen lone electron pair. The rate-determining step of the overall complexation is the entrance of the Na^+ into the ring with (possibly) concomitant rotation of the lone electron of the nitrogen to an endo configuration.

1. Introduction

Much work [1] has appeared recently on the kinetics of complexation of alkali metal cations with simple macrocycle crown ethers in a variety of solvents. The general Eigen-Winkler multistep mechanism:

$$Me^+ + C \underset{k_{-1}}{\overset{k_1}{\rightleftarrows}} Me^+ \cdots C \underset{k_{-2}}{\overset{k_2}{\rightleftarrows}} MeC^+ \underset{k_{-3}}{\overset{k_3}{\rightleftarrows}} (MeC)^+ \qquad (1)$$

appears adequate to describe the overall complexation process. In the above Me^+ is the alkali ion, C the free crown ether in solution, and $Me^+ \cdots C$ and MeC^+ two forms (solvent-separated and contact) of metal-macrocycle complexes, whereas (MeC^+) symbolizes the final complex formed with the cation embedded in the macrocycle cavity. The mechanism does not specify whether the rate-determining step of the process leading to (MeC^+) is the cation desolvation or the macrocyclic ligand rearrangement. This sort of information and its dependence on the nature of the solvent is sparse in the published literature [1]. An attempt has been made to place these ideas in focus in section 3. When subjected to careful comparison, the isomerization data clearly indicate the unique role of water, differentiating the rate-determining step of the complexation mechanism in water from that in the other solvents studied thus far.

The competition of the anion with solvent molecules and other ligands for cation coordination, even in solvents of intermediate dielectric permittivity, is reiterated. In solvents of low dielectric permittivity this role of the anion comes to dominate even for low donor number anions such as ClO_4^-, and a competition between anion and crown ether exists. In solvents of dielectric permittivity below 10, the cation is always paired with

Dedicated to Professor Manfred Eigen on the occasion of his 60th birthday.

Correspondence address: E.M. Eyring, Department of Chemistry, University of Utah, Salt Lake City, UT 84112, U.S.A.

the anion and represents the starting 'substrate' for the crown ether. The competition in this case is created by the dimerization of ion pairs and the interaction of an ion pair with the crown ether. These concepts are discussed in section 4. Interaction of alkali metal cations with monoazo crown ethers is discussed in section 5.

New data on the kinetics of isomerization of monoazo crown ethers (section 5) show that the rate-determining step of complexation corresponds to the entrance of Na^+ into the ring structure [2]. However, another relaxation at higher frequency exists. The hypothesis was advanced in a previous paper [2] that it corresponded to the rotation of the lone electron pair of the nitrogen atom in the ring with formation of a bond with the incoming metal cation. The idea that the inversion of the lone pair electrons of nitrogen is the source of the isomeric relaxations of the cryptand 222 has been used to account for experiments in aqueous solutions as well as in methanol and other protic solvents [3].

2. Experimental

The equipment for the ultrasonic work and the related procedure have been described elsewhere (refs. 1–3, including references cited therein).

Methoxyethoxyethylmonoazo 15C5 (RN15C5) and methylmonoazo 15C5 (MeN15C5) were synthesized at the University of Miami. Methanol was distilled over an Al amalgam. Solutions were prepared by weighing the crown ethers in volumetric flasks and adding methanol up to the mark. Contact with the open atmosphere in preparing the solutions and filling the ultrasonic cell was kept to a minimum (60–120 s total). The laboratory was air-conditioned thus maintaining a low relative humidity.

3. Mechanism of alkali metal cation complexation with simple crown ether: The role of the solvent

In previous relaxation kinetics studies the Eigen-Winkler multistep mechanism of eq. 1 above has been used successfully to describe ultrasonic data for alkali ions and Ba^{2+} reacting with crown ethers such as 18C6 in nonaqueous solvents such as dimethylformamide (DMF) and MeOH.

In DMF and MeOH it was found that the isomeric relaxation of the crown ether alone

$$C_1 \underset{k_{-0}}{\overset{k_0}{\rightleftarrows}} C_2 \tag{2}$$

is an overall process much faster than the last step of the Eigen-Winkler mechanism. This is true in the sense that the inverse of the relaxation time $\tau_0^{-1} = k_0 + k_{-0}$ is much larger than the reciprocal relaxation time for the metal complexation characterized by a 'slow' relaxation time τ_{II}. Previous similar findings by the temperature-jump relaxation technique [4] led to the formulation of the so-called Chock mechanism:

$$C_1 \underset{k_{-0}}{\overset{k_0}{\rightleftarrows}} C_2 \text{ (fast)},$$

$$Me^+ + C_2 \underset{k_r}{\overset{k_f}{\rightleftarrows}} MeC_2^+ \text{ (slow)}. \tag{3}$$

If one refers, however, to the rate constants rather than to the overall process and one realizes that $k_0 \ll k_{-0}$, it is apparent that in both DMF and MeOH $k_0 \simeq k_3$, namely, the slow isomeric step corresponds, in order of magnitude, to the last step of the metal cation complexation with 18C6 according to the Eigen-Winkler mechanism (eq. 1).

Hence, it seems that eq. 3 is not justified and that the Eigen-Winkler mechanism more correctly describes the actual process with the ligand rearrangement being the rate-determining step in the solvents MeOH and DMF. Confirmation of the above was obtained by increasing the rigidity of the ligand [5] using dihexano 18C6 and DB18C6 in DMF. As ligand rigidity increases the observed last process, characterized by τ_{II}, becomes much slower and, in many cases, its relaxation frequency lies below our measurable ultrasonic frequency range of approx. 1 to approx. 400 MHz.

These observations are different, however, from the results obtained previously in water for reactions between alkali metal cations and 18C6 [6] and 15C5 [7]. In these aqueous solution cases, it was shown that desolvation of the cation is the rate-determining step of the overall complexation reaction. In evaluating eq. 1, Eigen and Winkler [8] pointed out that the rate-determining step for the process could be the stepwise loss of an indeterminate number of solvent molecules from the first coordination sphere of the cation, a process concerted with a conformational rearrangement of the macrocycle ligand around the cation.

Obviously the 'event' that determines the overall rate in the concerted process may vary from ligand rearrangement to solvent substitution in the first coordination sphere of the cation depending on the relative energy barriers involved. For DMF and MeOH solvents, ligand rearrangement is rate limiting. For aqueous solutions cation desolvation seems to be rate limiting.

In order to put these ideas on a more quantitative basis, the existing isomerization data for 18C6 in water [9], DMF [1], MeOH [10] and EtOH [1b] are assembled in table 1 in terms of the available kinetic and thermodynamic parameters.

In table 1 the temperatures listed in row 1 refer to the temperature used in experiments for the isothermal portion of the original works [1,9,10].

In order to draw a comparison, values of the rate constant k_{-0} have been normalized to $t = -20\,^\circ\mathrm{C}$, although it is below the freezing point of water. It is evident that the normalized k_{-0} values in DMF, MeOH and EtOH denoted by k_{-0}^{ext} are comparable, hence they represent largely a property of the macrocycle. In contrast, the value of k_{-0}^{ext} in water is smaller by a factor of 3–4. Converse normalization to $t = 25\,^\circ\mathrm{C}$, assuming $\Delta H^{\neq}_{-0}$ and $\Delta S^{\neq}_{-0}$ to be temperature independent, gives row 8 in table 1 headed by the symbol $k_{-0}^{298.2}$. The value in water remains below those for the other solvents. There is experimental evidence [11] that suggests water may be incorporated inside the ring cavity of the macrocycle. This may explain the slower isomerization rate for aqueous 18C6.

We have also attempted a calculation of k_0 at 298.2 K in order to compare it with the k_3 of metal complexation, as noted above. From ΔG_0^t and ΔH_0 we have calculated ΔS_0. Then $\Delta G_0(298.2) = \Delta H_0 - 298.2\Delta S_0$ has been evaluated. From this we have calculated $K_0(298.2) = \exp(-\Delta G_0(298.2)/RT)$. This leads to $k_0 = k_{-0}K_0$ at $T = 298.2$ K denoted by k_0^{ext} (row 14 in table 1).

Although because of error propagation the calculation is rather inaccurate, it does show that a rough correlation exists between k_0 and k_3 for

Table 1

Kinetic and thermodynamic parameters and solvent properties for the isomeric equilibrium of 18C6 in solution

Solvent	Water [a]	DMF [b]	MeOH [c]	EtOH [d]
(1) t (°C)	25	-10	-20	-15
(2) k^t_{-0} (s^{-1})	6.2×10^8	5.5×10^8	3.1×10^8	4.8×10^8
(3) K_0^t	~ 0.02	6.5×10^{-3}	1×10^{-2}	4×10^{-3}
(4) k_0^t (s^{-1})	1×10^7	8.6×10^6	3.1×10^6	7.9×10^7
(5) $\Delta H^{\neq}_{-0}$ (kcal/mol)	7.4	7.5	5.8	4.8
(6) $\Delta S^{\neq}_{-0}$ (cal/K per mol)	7.7	10.2	3.5	~ 0
(7) k_{-0}^{ext} (253.2, s^{-1})	1×10^{-8}	3×10^8	3.1×10^8	3.8×10^8
(8) $k_{-0}^{298.2}$ (s^{-1})	6.2×10^8	3.3×10^9	2.0×10^9	1.9×10^9
(9) ΔG_0^t (kcal/mol)	2.3	2.6	2.3	2.83
(10) ΔH_0 (kcal/mol)	-2.6	-3.7	-2.6	-3.7
(11) ΔS_0 (cal/K per mol)	0 ± 0.02	-23.9	-19.4	-25.2
(12) ΔG_0^{298} (kcal/mol)	2.3	3.4	3.2	3.8
(13) K_0^{298}	0.02	3.2×10^{-3}	4.5×10^{-3}	1.6×10^{-3}
(14) k_0^{ext} (298.2, s^{-1})	1.2×10^7	1.1×10^7	9.0×10^6	6.2×10^5
(15) k_3 (s^{-1})	–	(K^+)9.1×10^6 [e]	(Na^+)1.1×10^7 [f]	–
(16) DN [g]	33	26.6	19	
(17) ε	78.5	36.7	32.66	24.2

$\Delta S_0 = -(\Delta G_0 - \Delta H_0)/T$. [a] Data from ref. 9. [b] Data from ref. 1. [c] Data from ref. 10. [d] Data from ref. 1b. [e] Data from ref. 13. [f] Data from ref. 5. [g] Donor number.

metal cation complexation in accord with eq. 1 for MeOH [5,9] and DMF [1] where a slower relaxation process for complexation was observable [5].

4. Macrocycle-anion competition for the solvated cation

One aspect that has attracted comparatively little attention [12] is the role of macrocycle-anion competition in the complexation process. Clearly, in principle, three ligands – solvent, anion and crown ether – all compete for the first coordination sphere sites around the cation. In a dynamic view of the process, the solvent is already coordinated around the cation (and presumably, albeit weakly, around the anion and also the crown ether). In a given solvent then one must consider anion-macrocycle competition for the cation as part of the successive steps leading to the metal-macrocycle complex. That the anion is able to compete with the macrocycle has been demonstrated [1] for LiSCN + 18C6 in DMF, since in this case no relaxation effect is observed that could be attributed to 18C6 attacking the LiSCN complex. The existence of complexation between Li^+ and SCN^- has been shown by an ultrasonic relaxation of LiSCN alone in DMF. $LiClO_4$ in DMF shows no relaxation [13], but a relaxation is observed [1] for $LiClO_4$ + 18C6 in DMF.

Similar results were obtained for the system $AgNO_3$ + 18C6 in DMF, showing effects quite distinct from those observed for $AgClO_4$ + 18C6 in DMF [14]. This was taken to indicate that NO_3^- competes with 18C6, thereby changing the amplitudes and the relaxation frequency of the ultrasonic relaxation spectrum of Ag^+ salts in DMF.

The anion becomes of paramount importance in media of low permittivity ($\varepsilon < 10$) where the electrolyte is present almost entirely in ion pairs at concentrations used for the ultrasonic work. Here the crown ether attacks a dipolar ion pair rather than the cation. The ion pair may participate in a dimerization equilibrium leading to quadrupoles according to the scheme:

$$\begin{aligned} &2\mathrm{MeX} \rightleftarrows (\mathrm{MeX})_2 \\ &\mathrm{MeX} + \mathrm{C} \rightleftarrows \mathrm{MeCX} \qquad (4) \end{aligned}$$

For instance, $LiClO_4$ is partially dimerized in 1,2-dimethoxyethane (DME) [15]. Addition of 18C6 causes a new relaxation to appear in accord with eq. 4.

On the other hand, $LiAsF_6$ in DME exists as ion pairs involved in a two-state equilibrium [16] with the solvated species LiS,AsF_6 in excess:

$$\mathrm{LiS,AsF_6} \rightleftarrows \mathrm{LiAsF_6} \qquad (5)$$

Addition of a crown ether, such as 18C6, causes a new process [17] to appear in competition with the above, according to the scheme:

$$\begin{aligned} &\mathrm{LiS,AsF_6} \rightleftarrows \mathrm{LiAsF_6} \\ &\mathrm{LiS,AsF_6} + \mathrm{C} \rightleftarrows \mathrm{LiC,\ AsF_6} \qquad (6) \end{aligned}$$

where the free solvent symbol S has been omitted from the right-hand side of the above reactions because it is present in large excess. Similarly, $LiClO_4$ in 2-methyltetrahydrofuran (2MeTHF) exists mainly as the dimer [18] $(LiClO_4)_2$ whereas $LiAsF_6$ is in an equilibrium between ion pairs and dimers [19].

For the same electrolyte and solvent, the macrocyclic cavity size and the nature of the crown ether have an effect on the rate of complexation as observed for $LiAsF_6$ + 12C4 and $LiAsF_6$ + 18C6 in DME [17]. No kinetic study of the effect of the cavity site on the anion competition, in media of low permittivity, has been carried out so far, to the knowledge of the present authors.

5. Interaction of metal cations with monoazo-tailed crown ethers: Isomeric equilibria of monoazo crown ethers

Recently, a study has been completed [2] of the kinetics of complexation of Na^+ ($NaClO_4$) in MeOH by a tailed crown ether ('lariat ether'), methoxyethoxyethylmonoazo 15C5 (**1**) and with methylmonoazo 15C5 (**2**).

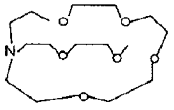

1

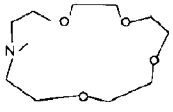

2

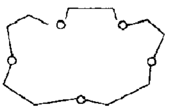

3

(7)

Species **3** is 15C5. A double relaxation was observed with both crown ethers **1** and **2** that was explained in terms of the multistep Eigen-Winkler scheme:

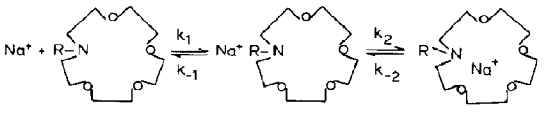

(8)

The presence of the side chain with its polar groups offers potentially an alternative coordination to the cation. This was judged to be unimportant, at least in terms of the appearance of an upper relaxation, since **2** shows the same double relaxation as **1** does. However, **1** shows a much larger overall stability constant for the complex than **2** does for Na^+ in MeOH, suggesting some participation of the chain in the coordination of Na^+.

The rate-determining step for the complexation process appears to be [2] the inclusion of the cation in the ring (probably concomitant with the rotation inward of the lone electron pair of nitrogen). Preliminary data, confirmed in the isomeric work reported below, showed [2] that the upper relaxation frequency for eq. 8 is comparable with the position of the isomeric relaxation of the crown ether alone. Since 15C5 (**3**) does not show any ultrasonic relaxation at the same temperature (298 K) at a comparable concentration (0.2 M) in MeOH as those shown by crown ethers **1** and **2**, the concentration-independent relaxation for crown ethers **1** and **2** in MeOH is attributed to the presence of nitrogen and to the inversion of its lone electron pair, an isomeric effect already found for 222 cryptand in water [3].

The faster ultrasonic relaxation of the solution containing metal ion plus azo crown ether is comparable in reciprocal frequency with the relaxation of the solution containing crown ether alone (although the latter is concentration independent, being a first-order process). This numerical correspondence suggests that the faster process in the electrolyte solutions corresponds to the rotation of the nitrogen and cation attack with the metal cation residing outside the cavity. The slower step would then correspond to the inclusion of the cation in the cavity of the macrocycle. The rotation of the side chain plays no major role in the isomerization process (energetically or entropically), since **1** shows a faster relaxation than **2** does despite the greater chain length in **1**. It is likely, however, that rotation of the chain occurs in the last step of metal complexation with extra coordination, since this would account for the larger stability constant of **1** compared to **2** for Na^+ complexation in MeOH at 25°C.

The above considerations make it interesting to determine the energy barrier to the isomerization of **1** and **2**. To this end a new ultrasonic study of the concentration and temperature dependence of the isomeric process has been carried out as shown below.

In figs. 1 and 2 the ultrasonic spectra expressed as the excess sound absorption per wavelength $\alpha_{exc}\lambda = \mu = (\alpha - Bf^2)(u/f)$ vs. the frequency f are depicted for two representative concentrations of **1** and **2** in MeOH. Here, α is the sound attenuation coefficient (neper cm^{-1}), B denotes values of α/f^2 for frequencies above the relaxation frequency f_r, and u is the sound velocity. The solid lines in figs. 1 and 2 correspond to the fitted Debye function for a single relaxation process

$$\mu = 2\mu_{max}\frac{f/f_r}{1 + (f/f_r)^2} \tag{9}$$

where μ_{max} is the value of μ at $f = f_r$.

Table 2 reports at all the concentrations and temperatures investigated for **1** and **2** the relaxation parameters μ_m, f_r and B, and the sound velocity u. The parameter B is determined by fitting α and f data to the Debye function for a single relaxation process:

$$\frac{\alpha}{f^2} = \frac{A}{1 + (f/f_r)^2} + B \tag{10}$$

with

$$A = (2\mu_{max}/u \cdot f_r) \tag{11}$$

For a single isomeric process

$$C_1 \underset{k_{-0}}{\overset{k_0}{\rightleftarrows}} C_2 \tag{12}$$

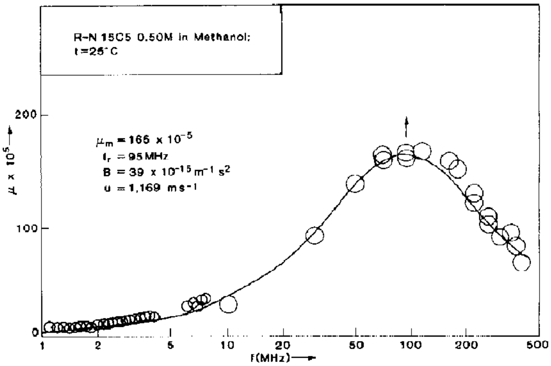

Fig. 1. Representative ultrasonic relaxation spectrum for RN15C5 in MeOH at 25° C, expressed as μ vs. f. (———) Fitted Debye function for a single relaxation process (eq. 10).

the following equations hold [1]:

$$\tau^{-1} = k_{-0}(1 + K_0) = \frac{kT}{h}\left(e^{\Delta S^{\neq}_{-0}/R}\right)\left(e^{-\Delta H^{\neq}_{-0}/RT}\right) \times (1 + K_0) \tag{13}$$

$$\frac{\mathrm{d}\ln(\tau^{-1}/T)}{\mathrm{d}(1/T)} = -\frac{\Delta H^{\neq}_{-0}}{R} - \frac{K_0}{1 + K_0} \cdot \frac{\Delta H_0}{R} \tag{14}$$

$$\mu_{\mathrm{m}} = \frac{\pi}{2\beta_{\mathrm{s}}} \cdot \frac{\Delta V_{\mathrm{s}}^2}{RT} \cdot \frac{K_0}{(1 + K_0)^2} \cdot C \tag{15}$$

$$\frac{\mathrm{d}\ln(\mu_{\mathrm{m}}T/u^2)}{\mathrm{d}(1/T)} = \frac{\Delta H_0}{R} \cdot \frac{K_0 - 1}{K_0 + 1} \tag{16}$$

where $K_0 = k_0/k_{-0}$; $\Delta H^{\neq}_{-0}$ and $\Delta S^{\neq}_{-0}$ are the enthalpy and entropy of activation for the reverse process. ΔV_{s} is the isoentropic volume change of reaction 12, and $\beta_{\mathrm{s}} = (\rho u^2)^{-1}$ is the adiabatic compressibility.

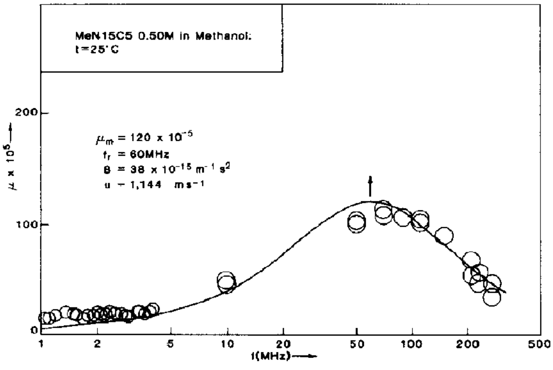

Fig. 2. Representative ultrasonic relaxation spectrum for MeN15C5 in MeOH at 25° C, expressed as μ vs. f. (———) Fitted Debye function for a single relaxation process (eq. 10).

Plots of eqs. 14–16 with the solid lines calculated by linear regression are shown for **1** and **2** in MeOH in figs. 3 and 4, respectively.

For crown ether **1**, linear regression applied to the data of eq. 14 gives: determination coefficient $r^2 = 0.98$, intercept $I = 19.4_5$, slope $= S = -147_7$, hence $\Delta S^{\neq}_{-0} = -8.6$ cal/K per mol ($\Delta S^{\neq}_{-0} = R(-\ln(k/h) + I)$). Linear regression applied to the data of eq. 16 gives $r^2 = 0.82$, $I = -28.47$ and $S = 1181$. Then from table 2, given $\tau^{-1} = 5.6_5 \times 10^8$ s^{-1} at 248 K, one writes:

$$5.6_5 \times 10^8 = kT/h\left(e^{\Delta S^{\neq}_{-0}/R}\right)\left(e^{-\Delta H^{\neq}_{-0}/RT}\right)(1 + K_0)$$

$$1477 = \frac{\Delta H^{\neq}_{-0}}{R} + \frac{K_0}{1 + K_0} \cdot \frac{\Delta H_0}{R} \tag{17}$$

$$1181 = \frac{\Delta H_0}{R} \cdot \frac{K_0 - 1}{K_0 + 1}$$

leading (by using the value of $\Delta S^{\neq}_{-0} = -8.6$ cal/K per mol) to the transcendental equation:

$$6.91 \times 10^{-3} = \left\{\exp\left[-\left(1477 - 1181\frac{K_0}{K_0 - 1}\right)\frac{1}{T}\right]\right\} \times (1 + K_0) \tag{18}$$

which has a solution for $K_0 = 7 \times 10^{-3} \ll 1$.

Eqs. 17 then with $K_0 \ll 1$ give the kinetic and thermodynamic parameters collected in table 3.

For crown ether **2**, linear regression applied to the data of eq. 14 gives: $r^2 = 0.96$, $I = 19.05$ and $S = -1527$ from which $\Delta S^{\neq}_{-0} = -9.4$ cal/K per mol.

For crown ether **2**, linear regression applied to the data of eq. 16 gives $r^2 = 0.47$, $I = -27.02$ and $S = 700$.

Then, from table 2, given $\tau^{-1} = 3.4_6 \times 10^8$ s^{-1} at $T = 298$ K, one writes:

$$3.4_6 \times 10^8 = \frac{kT}{h}\left(e^{\Delta S^{\neq}_{-0}/R}\right)\left(e^{-\Delta H^{\neq}_{-0}/RT}\right)(1 + K_0)$$

$$1527 = \frac{\Delta H^{\neq}_{-0}}{R} + \frac{K_0}{1 + K_0} \cdot \frac{\Delta H_0}{R} \tag{19}$$

$$700 = \frac{\Delta H_0}{R} \cdot \frac{K_0 - 1}{K_0 + 1}$$

Table 2

Ultrasonic parameters (f_r, μ_m, B) and sound velocity (u) for the isomeric relaxation of crown ethers **1** and **2** in MeOH at the concentrations C (M = mol/dm^3) and temperatures t (°C) indicated

The parameters f_r and μ_m are affected by an average error of ±5%, B is uncertain within 1×10^{-17} cm^{-1} s^2 and u is affected by an average error of ±1%. The last digit of the velocity is reported in order to avoid round-off errors in future recalculations from the present data.

t (°C)	C (M)	f_r (MHz)	μ_m ($\times 10^5$)	B ($\times 10^{-17}$) (cm^{-1} s^2)	u ($\times 10^{5}$) (cm s^{-1})
Crown ether **1**					
25	0.50	95	165	39	1.169
25	0.40	90	110	37	1.149
25	0.30	90	90	38	1.143
25	0.20	80	55	33.5	1.127
25	0.20	90	70	33	1.142
15	0.30	80	140	35	1.166
0	0.30	55	180	39	1.219
−7	0.30	45	200	42.5	1.242
Crown ether **2**					
25	0.50	60	120	38	1.144
25	0.40	50	95	36	1.127
25	0.30	60	75	34	1.138
25	0.20	50	65	33	1.138
15	0.30	40	84	36	1.165
5	0.31	35	130	37	1.201
−5	0.31	27	131	38	1.240

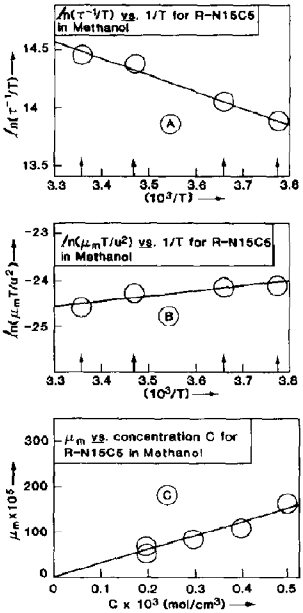

Fig. 3. (A) $\ln(\tau^{-1}/T)$ vs. $1/T$ for RN15C5 in MeOH. (B) $\ln(\mu_m T/u^2)$ vs. $1/T$ for RN15C5 in MeOH. (C) μ_m vs. C for RN15C5 in MeOH at 25°C.

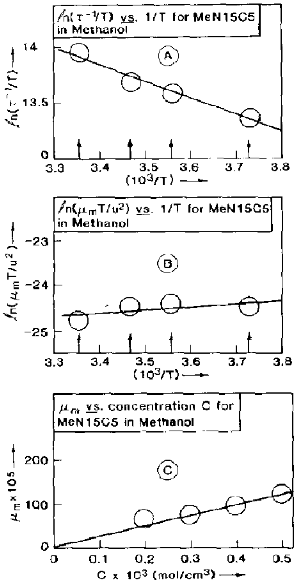

Fig. 4. (A) $\ln(\tau^{-1}/T)$ vs. $1/T$ for MeN15C5 in MeOH. (B) $\ln(\mu_m T/u^2)$ vs. $1/T$ for MeN15C5 in MeOH. (C) μ_m vs. C for MeN15C5 in MeOH at 25°C.

Table 3

Kinetic and thermodynamic parameters for the isomeric relaxation of crown ethers **1** and **2** in MeOH

	Crown ether **1**	Crown ether **2**
T (K)	298.2	298.2
k_{-0} ($\times 10^8$) (s^{-1})	5.6_5	3.5
K_0	$\ll 1$	$\ll 1$
$\Delta S^{\neq}_{-0}$ (cal/K per mol)	−8.6	$-9._4$
$\Delta H^{\neq}_{-0}$ (kcal/mol)	2.9_3	3.0
ΔH_0 (kcal/mol)	−2.4	−1.4
$\Delta H_0^{\neq}$ (kcal/mol)	0.5	1.6

leading (by using the value of $\Delta S^{\neq}_{-0} = -9.4$ cal/K per mol) to the transcendental equation:

$$6.33 \times 10^{-7} = \left\{\exp\left[-\left(1527 - 700\frac{K_0}{K_0 - 1}\right)\frac{1}{T}\right\}\right. \times (1 + K_0) \qquad (20)$$

which has a solution for $K_0 \ll 1$.

Eqs. 19 then with $K_0 \ll 1$ give the kinetic and thermodynamic parameters collected in table 3.

Analysis of table 3 reveals that the observed difference between the τ values arises largely from the entropy of activation $\Delta S^{\neq}_{-0}$, the enthalpies of activation being quite close. The similarity of the activation enthalpies is clear from figs. 3 and 4 in which the slopes of $\ln(\tau^{-1}/T)$ vs. $1/T$ are comparable. As $k_{-0} \gg k_0$ and $\Delta S^{\neq}_{-0} < 0$, one would be tempted to speculate that the fast step in the isomerisation leads to solvation of the crown ether with increased order in the activated state and that the slow step corresponding to k_0 involves desolvation. From the point of view of nitrogen inversion this would correspond to the formation of a solvated exo configuration for the reverse process and to an endo configuration for the forward process in

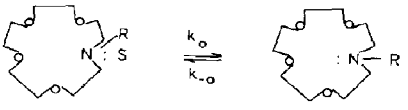

6. Conclusion

Introduction of nitrogen into the crown ether ring with an aliphatic ether tail on the nitrogen has an interesting consequence. The rotation of the lone pair of electrons of nitrogen plays a major role in determining the position, on the frequency axis, of the upper relaxation frequency when such a crown ether reacts with Na^+. The entrance of Na^+ into the ring with probable rotation of the lone electron pair inward (endo configuration) remains the rate-determining step of complexation. Extension of this work to other cations should clear up the relative importance of ring rearrangement and nitrogen atom rotation to the activation energy profile of the complexation reaction. As for the isomeric relaxation studied in the present work, the reverse rate depends somewhat entropically on the presence of the side chain of the present N-pivot lariat crown ethers. It should prove interesting to study similar crown ethers having changes in the structure of the tail and to observe their effect on the complexation reaction profile.

Acknowledgement

This work was funded by the National Science Foundation (Grant CHE-8513266).

References

1 a K.J. Maynard, D.E. Irish, E.M. Eyring and S. Petrucci, J. Phys. Chem. 88 (1984) 729; b C. Chen, W. Wallace, E.M. Eyring and S. Petrucci, J. Phys. Chem. 88 (1984) 2541.

2 G.W. Gokel, L. Echegoyen, M.S. Kim, E.M. Eyring and S. Petrucci, J. Phys. Chem. (1987) submitted for publication.

3 a H. Schneider, S. Rauh and S. Petrucci, J. Phys. Chem. 85 (1981) 2287; b F. Eggers, T. Funck, H. Richman, H. Schneider, E.M. Eyring and S. Petrucci, J. Phys. Chem. (1987) in the press.

4 P.B. Chock, Proc. Natl. Acad. Sci. U.S.A. 69 (1972) 1939.

5 W. Wallace, C. Chen, E.M. Eyring and S. Petrucci, J. Phys. Chem. 89 (1985) 1357.

6 a G.W. Liesegang, M.M. Farrow, N. Purdie and E.M. Eyring, J. Am. Chem. Soc. 98 (1976) 6905; b G.W. Liesegang, M.M. Farrow, F.A. Vazquez, N. Purdie and E.M. Eyring, J. Am. Chem. Soc. 99 (1977) 3240.

7 L.J. Rodriguez, G.W. Liesegang, R.D. White, M.M. Farrow, N. Purdie and E.M. Eyring, J. Phys. Chem. 81 (1977) 2118.

8 M. Eigen and R.M. Winkler, in: Neurosciences second study program, ed. F.O. Schmitt (Rockefeller University Press, New York, NY, 1970) p. 685.

9 G.W. Liesegang, M.M. Farrow, L.J. Rodriguez, R.K. Burnham and E.M. Eyring, Int. J. Chem. Kin. 10 (1978) 471.

10 C. Chen and S. Petrucci, J. Phys. Chem. 86 (1982) 2601.

11 W.P. McKenna and E.M. Eyring, Appl. Spectrosc. 40 (1986) 20.

12 N.S. Poonia and A.V. Bajaj, Chem. Rev. 79 (1979) 389.

13 C. Chen, W. Wallace, E.M. Eyring and S. Petrucci, J. Phys. Chem. 88 (1984) 2541.

14 S. Petrucci, R.J. Adamic and E.M. Eyring, J. Phys. Chem. 90 (1986) 1677.

15 a S. Onishi, H. Farber and S. Petrucci, J. Phys. Chem. 84 (1980) 2922; b H. Farber and S. Petrucci, J. Phys. Chem. 85 (1981) 1396.

16 H. Farber, D.E. Irish and S. Petrucci, J. Phys. Chem. 87 (1983) 3515.

17 H. Richman, Y. Harada, E.M. Eyring and S. Petrucci, J. Phys. Chem. 89 (1985) 2373.

18 H. Maaser, Ph.D. Thesis, Rutgers University, Newark NJ (1982).

19 M. Delsignore, H. Maaser and S. Petrucci, J. Phys. Chem. 88 (1984) 2405.